Mapping of RNA modifications by direct Nanopore sequencing and JACUSA2

Amina Lemsara[1,2], Christoph Dieterich[*1,2,3], and Isabel Naarmann-de Vries[1,2,3]

[1]Klaus Tschira Institute for Integrative Computational Cardiology, University Heidelberg, 69120 Heidelberg, Germany
[2]Department of Internal Medicine III (Cardiology, Angiology, and Pneumology), University Hospital Heidelberg, 69120 Heidelberg, Germany
[3]German Centre for Cardiovascular Research (DZHK)-Partner Site Heidelberg/Mannheim, 69120 Heidelberg, Germany

Abstract

RNA modifications exist in all kingdom of life. Several different types of base or ribose modifications are now summarized under the term the "epitranscriptome". With the advent of high-throughput sequencing technologies much progress has been made in understanding RNA modification biology and how these modifications can influence many aspects of RNA life. The most widespread internal modification on mRNA is m6A, which has been implicated in physiological processes as well as disease pathogenesis. Here, we provide a workflow for the mapping of m6A sites using Nanopore direct RNA sequencing data. Our strategy employs pairwise comparison of base calling error profiles with JACUSA2. We outline a general strategy for RNA modification detection on mRNA and describe two specific use cases on m6A detection in detail. **Use case 1:** a sample of interest with modifications (e.g. "wild type" sample) is compared to a sample lacking a specific modification type (e.g. "knock out" sample, here *METTL3*-KO) or **Use case 2:** a sample of interest with modifications is compared to a sample lacking all modifications (e.g. *in vitro* transcribed cDNA). We provide a detailed protocol on experimental and computational aspects. Extensive online material provides a snakemake pipeline to identify m6A positions in mRNA and to validate the results against a miCLIP-derived m6A reference set. The general strategy is flexible and can be easily adapted by users in different application scenarios.

---

[*]Correspondence to: christoph.dieterich@uni-heidelberg.de

INTRODUCTION

Chemical modifications on DNA and histones, also known as epigenetics marks, strongly impact gene expression during cell differentiation and in several other biological programs. In the 1970s, it was recognized that RNA is also subjected to extensive covalent modification, and studies in the late 1980s revealed the widespread deamination of bases (termed RNA editing), which can lead to recoding if it occurs within coding sequences. Impressive development in the RNA modification field occurred during the past eight years, with the discovery of an extensive layer of base modifications in mRNAs. These can influence gene expression and have been already shown to be involved in primary cellular programs such as stem cell differentiation, response to stress, and the circadian clock. The study of RNA modifications and their effects is now referred to as epitranscriptomics, and it reveals striking similarities to what is known for epigenomics. To date thirteen distinct modifications have been identified on mRNA transcripts [Anreiter et al., 2021]. These modifications are catalyzed by a variety of dedicated enzymes and can be divided into two classes: modifications of cap-adjacent nucleotides and internal modifications.

In contrast to the m7G cap, the impact of internal modifications on gene regulation has been less studied apart from RNA editing, which is mediated by RNA deaminases (e.g. the ADAR family). The most widespread internal mRNA modification is N6-methyladenosine (m6A). By modulating the processing of mRNA, m6A can regulate a wide range of physiological processes and its alteration has been linked to several diseases Roignant and Soller [2017], Zaccara et al. [2019], Shi et al. [2019]. The modification is catalyzed co-transcriptionally by a Mega-Dalton methyltransferase complex, which includes the heterodimer METTL3-METTL14 and other associated subunits Garcias Morales and Reyes [2021]. This modification is reversible since two proteins of the AlkB-family of demethylases can remove m6A from mRNA transcripts [Jia et al., 2011, Zheng et al., 2013]. In mammals, m6A preferentially localizes within long internal exons and at the beginning of terminal exons at so-called DRACH motif (D = A/G/U, R = A/G, H = A/C/U) sites [Dominissini et al., 2012, Meyer et al., 2012, Ke et al., 2015]. Once deposited, m6A is recognized by several reader proteins that can affect the fate of mRNA transcripts in nearly every step of the mRNA life cycle, including alternative splicing [Adhikari et al., 2016, Roundtree et al., 2017], mRNA translation [Wang et al., 2015] and decay [Wang et al., 2014, Du et al., 2016, Roundtree et al., 2017]. The best-described readers are the YTH domain family of proteins that decode the signal and mediate m6A functions. By affecting RNA structure, m6A can also indirectly influence the association of additional RNA-binding proteins (RBPs) and the assembly of larger messenger ribonucleoprotein particles (mRNPs) [Patil et al., 2018].

Several approaches have been presented to map RNA modifications on RNA. Herein, we focus on mRNA modification site detection in general and on m6A in particular where antibody-based protocols (miCLIP), methylation-sensitive restriction enzyme assays (MazF) or transgenic approaches (TRIBE, DART) have been presented to map m6A sites. All of the aforementioned approaches rely on high-throughput short read sequencing on the Illumina platform. This typically involves cDNA synthesis by reverse transcription and PCR-based library amplification. One recent addition to the toolbox of RNA modification mapping is direct RNA single molecule long read sequencing on the Oxford Nanopore Technologies platform (dRNA-seq). While our software is able to deal with Illumina and Nanopore-based approaches, the latter is the principal topic of this methods article.

MATERIALS

ONT direct RNA sequencing

This section summarizes all necessary consumables for direct RNA sequencing of poly-adenylated RNA (i.e. mRNA) on the MinION or similar device.

1. 500 ng polyA$^+$ RNA isolated from total RNA e.g. with Oligotex mRNA kit (#70022, Qiagen) or Dynabeads oligo dT$_{25}$ beads (#61002, Thermo Fisher Scientific) or *in vitro* transcriptome sample. Store RNA at -80 °C and the mRNA purification kit as recommended by the manufacturer.

2. Nuclease-free water. Store at room temperature.

3. Direct RNA-sequencing kit (SQK-RNA002, Oxford Nanopore Technologies). Store at -20 °C.

4. NEBNext Quick Ligation Reaction Buffer (#B6058S, New England Biolabs). Store at -20 °C.

5. T4 DNA Ligase (#M0202S, New England Biolabs). Store at -20 °C.

6. dNTP Mix (10 mM each, #R0191, Thermo Fisher Scientific). Store at -20 °C.

7. SuperScript IV Reverse Transcriptase (#18090010, Thermo Fisher Scientific). Store at -20 °C.

8. Agencourt RNAClean XP beads (#A63987, Beckman Coulter). Store at 4 °C.

9. 70 % ethanol, freshly prepared.

10. Qubit dsDNA HS assay kit (#Q32854) and Qubit Fluorometer (Thermo Fisher Scientific).

11. Flow cell priming kit (EXP-FLP002, Oxford Nanopore Technologies). Store at -20 °C.

12. Thermocycler.

13. Gentle rotator mixer.

14. Magnetic stand for 1.5 ml tubes.

15. 1.5 ml DNA LoBind tubes (Eppendorf), 0.2 ml PCR tubes.

16. MinION or GridION sequencing device and MinION R9.4.1 Flow cells (FLO-MIN106D, Oxford Nanopore Technologies). Store Flow cells at 4 °C.

Preparation of an *in vitro* transcriptome sample

1. 100 ng polyA$^+$ RNA isolated from total RNA e.g. with Oligotex mRNA kit (#70022, Qiagen) or Dynabeads oligo dT$_{25}$ beads (#61002, Thermo Fisher Scientific). Store RNA at -80 °C and the mRNA purification kit as recommended by the manufacturer

2. 10 μM oligo(dT)-VN RT primer.

   TTTTTTTTTTTTTTTTTTTTTTTTTTTTTTVN. Store at -20 °C.

3. 20 μM template switching oligo (TSO). ACTCTAATACGACTCAC-TATAGGGAGAGGGCrGrG+G. Store at -20 °C.

4. 10 μM T7 extension primer. GCTCTAATACGACTCACTATAGG. Store at -20 °C.

5. Nuclease-free water. Store at room temperature.

6. dNTP Mix (10 mM each, #R0191, Thermo Fisher Scientific). Store at -20 °C.

7. Template Switching RT Enzyme Mix (#M0466S, New England Biolabs). Store at -20 °C.

8. Q5 Hot Start High-Fidelity 2X Master Mix (#M0494S, New England Biolabs). Store at -20 °C.

9. RNase H (5,000 U/ml) (#M0297S, New England Biolabs). Store at -20 °C.

10. NucleoSpin Gel and PCR Clean-up, Mini kit for gel extraction and PCR clean up (#740609.50, Macherey-Nagel) or equivalent. Store at room temperature.

11. MEGAscript T7 transcription kit (#AM1334, Thermo Fisher Scientific). Store at -20 °C.

12. RNA Clean & Concentrator-25 kit (#R1017, Zymo Research). Store at room temperature.

13. Thermocycler.

14. Table top centrifuge for 1.5 ml tubes.

15. Nanodrop spectrophotometer or equivalent.

16. 0.2 ml PCR tubes, 1.5 ml DNA LoBind tubes (Eppendorf).

Hardware requirements

All analyses have been performed/tested on two alternative hardware systems: a standard Linux desktop computer or an Apple iMac (Retina 5K, ultimo 2014). The workflow requires a multi-core processor system with minimal main memory of 16GB RAM and several GBs of free disk space (depending on data set size).

Software dependencies and installation

Our analysis workflow has few requirements, which are detailed in Table 1. Specifically, to execute our workflow, the following prerequisites are necessary: a BASH shell, a JAVA runtime environment, a working PERL and R installation. Additional i.e. non-standard software to process and map Nanopore reads (bedtools, samtools and Minimap2) are obligatory. Table 2 lists some additional R packages, which are required to run the R code. Detailed installation instructions and corresponding workflow code are deposited under `https://github.com/dieterich-lab/MiMB_JACUSA2_chapter`.

METHODS

Our workflow is based on the pairwise comparison of samples with different modification status (Figure 1). The sample of interest (yellow) may be compared to different samples lacking certain modifications. If available, the wild type (WT) sample can be compared to a knock out (KO) sample lacking specific enzymatic activities (green), as outlined in Use Case 1. Alternatively, a sample lacking all modifications may be used for comparison

(blue). This may be either a simulated sample (i.e. with NanoSim) or an *in vitro* transcribed sample derived from cDNA. Such an analysis is detailed in Use Case 2. In any setting, JACUSA2 calculates scores for the Mismatch, Insertion and Deletion rates of the pairwise comparisons as outlined above (Figure 1, right).

One feature of Nanopore sequencing is to read sequences as 5-mers, as always five nucleotides are occupied by the pore protein (Figure 2). Because of this, a m6A modification may affect basecalling not only if the modified nucleotide is in the central position, but also at neighboring positions (-2 to +2). To account for this, JACUSA2 scores for Deletion, Mismatch and Insertion are calculated for the entire 5-mer context. Depending on the modification-specific signature, a Feature set can be selected to calculate the final JACUSA2 score (Figure 2).

Our workflow can be divided into a wet-lab part (Figure 3A) and a computational part (Figure 3B). Starting from total cellular RNA, polyA$^+$ RNA is isolated and subjected to Nanopore direct RNA-sequencing. Guppy basecalling can be done as well as live basecalling during sequencing on the respective FAST5 files, which results in FASTQ output files (Figure 3A). FASTQ files are aligned to a reference sequence with Minimap2. SAMtools is used to generate BAM files as input for JACUSA2 analysis, which yields candidate m6A sites with the presented workflow in this chapter (Figure 3B). We will present all necessary experimental step for dRNA-seq in the next section.

Nanopore direct RNA sequencing

1. Adjust 500 ng polyA$^+$ RNA to a total volume of 9 μl with nuclease-free water. Complete RT adapter ligation reaction (in 0.2 ml PCR tube) with 3 μl NEBNext Quick Ligation Reaction Buffer, 0.5 μl RNA CS (RCS, from SQK-RNA002), 1 μl RT-Adapter (RTA, from SQK-RNA002) and 1.5 μl T4 DNA Ligase. Incubate 10 min at room temperature.

2. Prepare reverse transcription master mix on ice during ligation: 9 μl nuclease-free water, 2 μl 10 mM dNTPs, 8 μl 5x SuperScript IV first strand buffer, 4 μl 0.1 mM DTT.

3. Add the reverse transcription master mix to the ligation reaction and mix by pipetting. Add 2 μl SuperScript IV reverse transcriptase and mix by pipetting. Incubate in a thermocycler with the following protocol: 50 min at 50 °C, 10 min at 70 °C, cool down to 4 °C.

4. Let the Agencourt RNAClean XP beads come to room temperature during reverse transcription. Carefully resuspend beads before use. Transfer reaction to a 1.5 ml DNA LoBind tube and mix with 72 μl

Agencourt RNAClean XP beads. Incubate 5 min at room temperature on a gentle rotator mixer.

5. Collect beads on a magnetic stand and remove supernatant. Wash pelleted beads two times (30 sec) with 200 μl freshly prepared 70 % ethanol. Remove supernatant. Spin sample down and place on magnet again. Remove any residual ethanol.

6. Resuspend beads in 20 μl nuclease-free water by gentle flicking and incubate 5 min at room temperature on a gentle rotator mixer. Collect beads on a magnetic stand and transfer 20 μl eluate in a fresh 1.5 ml DNA LoBind tube.

7. For ligation of the RMX adapter, add the following to 20 μl eluate: 8 μl NEBNext Quick Ligation Reaction Buffer, 6 μl RMX (from SQK-RNA002), 3 μl nuclease-free water, 3 μl T4 DNA Ligase. Mix by pipetting and incubate 10 min at room temperature.

8. Add 40 μl carefully resuspended Agencourt RNAClean XP beads to the reaction and mix by pipetting. Incubate 5 min at room temperature on a gentle rotator mixer.

9. Collect beads on a magnetic stand and remove supernatant. Wash pelleted beads two times with 150 μl wash buffer (WSB, from SQK-RNA002). Resuspend beads by flicking, spin down and return to magnetic stand. Remove supernatant from pelleted beads.

10. Resuspend beads in 21 μl elution buffer (EB, from SQK-RNA002) by gentle flicking and incubate 5 min at room temperature on a gentle rotator mixer. Pellet beads on a magnetic stand and transfer 21 μl eluate in a fresh 1.5 ml DNA LoBind tube.

11. Quantify 1 μl of the library on a Qubit fluorometer with the Qubit dsDNA HS kit according to the manufacturerers protocol. Concentration should be usually in the range of 5 - 10 ng/μl.

12. Insert MinION R9.4.1 Flow cell in the MinION or GridION sequencing device and perform Flow cell check in the MinKNOW software. For successful sequencing of mammalian polyA$^+$ RNA at least 1,000 available pores are recommended.

13. Prepare Priming Mix by adding 30 μl flush tether (FLT, from EXP-FLP002) to a vial of flush buffer (FB, from EXP-FLP002) and mix by pipetting. Open priming port. Remove air bubble from priming port by inserting the tip of a P1000 pipette into the priming port and slowly dialing up, until a small volume of storage buffer enters the pipette tip. Load 800 μl Priming Mix via the priming port and carefully avoid introduction of air bubbles. Close the priming port and wait for 5 min.

14. Mix 20 μl library with 17.5 μl nuclease-free water and 37.5 μl RNA running buffer (RRB, from SQK-RNA002) and mix by pipetting. Open the priming port and the sample port. Load 200 μl Priming Mix via the priming port. Mix library by pipetting just before loading and load dropwise via the sample port. Carefully avoid introduction of air bubbles. Close the sample port and the priming port.

15. Start sequencing for 48 to 72 h in the MinKNOW software. Choose direct RNA-sequencing kit and high-accuracy basecalling as parameters.

Preparation of an *in vitro* transcriptome sample

The *in vitro* transcriptome sample is prepared based on a protocol published by Zhang et al. [2021] with some modifications a detailed below. An *in vitro* transcriptome lacks any RNA modifications and is a perfect reference sample for RNA modification mining.

1. Adjust 100 ng polyA$^+$ RNA to a total volume of 6 μl with nuclease-free water. Add 1 μl each of 10 μM oligo(dT)-VN RT primer and 10 mM dNTPs. Mix by pipetting and incubate in a thermocycler: 5 min at 75 °C, 2 min at 42 °C, cool to 4 °C.

2. Assemble 2.5 μl 4x template switching RT buffer, 0.5 μl 20 μM TSO, 1 μl 10x template switching RT enzyme mix and mix by pipetting. Combine with 6 μl RNA and incubate in a thermocycler: 90 min at 42 °C, 10 min at 68 °C, cool to 4 °C.

3. For Second strand synthesis add to First strand synthesis reaction: 50 μl Q5 Hot Start High-Fidelity 2X Master Mix, 5 μl RNase H, 2 μl 10 μM T7 extension primer, 33 μl nuclease-free water. Mix by pipetting and incubate in a thermocycler: 15 min at 37 °C, 1 min at 95 °C, 10 min at 65 °C, cool to 4 °C.

4. Purify double stranded cDNA with NucleoSpin Gel and PCR Clean-up kit according to the manufacturerers protocol and elute in 20 μl elution buffer. Determine concentration on a Nanodrop spectrophotometer. cDNA may be stored at -20 °C.

5. Combine 8 μl cDNA for *in vitro* transcription with 2 μl each of ATP, GTP, CTP, UTP, 10x reaction buffer and enzyme mix from the MEGAscript T7 transcription kit. Incubate 3 h at 37 °C.

6. Digest template DNA by addition of 1 μl Turbo DNase. Mix by pipetting and incubate 15 min at 37 °C.

7. Adjust reaction volume to 100 μl with nuclease-free water and clean up with RNA Clean & Concentrator-25 kit according to the manufacturers protocol, using two volumes of adjusted RNA binding buffer (1:1 RNA binding buffer : ethanol). Elute RNA in 25 μl nuclease-free water. Determine RNA concentration on a Nanodrop spectrophotometer. Store at -80 °C.

Nanopore read processing

1. Base call the ionic current signal stored in FAST5 files using Guppy. For the IVT sample, we applied real-time base calling with the MinKNOW-embedded Guppy basecaller. Otherwise, Guppy basecaller software can be used. In this case, the basecaller requires the path to FAST5 files, the output folder, and the config file or the flowcell/kit combination. The output are FASTQ files that can be compressed using the option "–compress_fastq".

   ```
   $ guppy_basecaller --compress_fastq -i path_to_fast5 -s path_to_output
   -c config_file.cfg --cpu_threads_per_caller 14 --num_callers
   1
   ```

   Set the number of threads "cpu_threads_per_caller" and the number of parallel basecallers "num_caller" according to your resources. Additional details can be found at https://nanoporetech.com/.

2. Align reads to the transcriptome using Minimap2 software. The output is a SAM file that has to be converted to a compressed form as BAM file using SAMtools command. The alignment requires a reference sequence. Here, we used GRCh38 Ensembl release 96 annotation and FASTA file. Pre-indexing of the human genome saves time during read alignment. Please save the index with the option "-d" before read mapping and use the index instead of the reference file in the minimap2 command line.

   ```
   $ minimap2 -d reference.mmi reference.fa
   ```

   For Direct RNA Sequencing, it is recommended to set a small k-mer size "-k [=14]" to enhance sensitivity. We recommend outputting only primary alignments "–secondary=no". Use the parameter '–MD' to add the reference sequence information to the alignment; this is necessary for JACUSA2 downstream analysis. Adjust the number of threads "-t" according to your resources. Check Minimap2 manual for more details [Min]. To enable spliced alignments, use the setting -ax splice –junc-bed annotation.bed –junc-bonus where "–junc-bonus" allows to tune the bonus score and the BED file "–junc-bed annotation.bed" provides the splice junctions.

```
$ minimap2 -t 5 --MD -ax splice --junc-bonus 1 -k14 --secondary=no
--junc-bed final_annotation_96.bed -ub reference.mmi Reads.fastq.gz
|samtools view -bS > mapping.bam
```

The BED file can be generated from EnsEMBL GTF files using the
following command:

```
$paftools.js gff2bed annotation.gtf > annotation.bed
```

3. Mapping RNA modifications using JACUSA2 pipeline: JACUSA2
   [Piechotta et al., 2021] rapidly detects RNA modifications based on
   a comparative strategy where read alignment features (mismatch, in-
   sertion and deletion) of samples of interest are compared to a reference
   sequence (call-1) or against reference samples without the correspond-
   ing RNA modification of interest (call-2). JACUSA2 processes repli-
   cate experiments. The analysis of read alignment signatures is used
   for RNA modification detection. Particularly, we integrate JACUSA2
   call-2 method with the downstream analysis in one workflow using
   the Snakemake workflow manager [Köster and Rahmann, 2012]. Our
   Snakemake workflow encompasses several steps as shown in Figure
   4. The workflow requires BAM files from 2 conditions as input. We
   suggest to filter secondary and poor alignments beforehand. The out-
   put of JACUSA2 call2 is preprocessed (get_features) and subjected
   to a machine learning step to extract and visualize modification pat-
   terns (resp. get_pattern, visualize_pattern) and make predictions (pre-
   dict_modification). "split_trani_test" rule allows splitting input data
   into a training set and a test set. To use our snakemake-based JA-
   CUSA2 pipeline a set of parameters should be defined in the "con-
   fig.yaml" file; mainly: the label of the analysis 'label', the input bam
   files under 'data', the reference sequence 'reference', a file containing
   size of chromosomes 'chr_size', JACUSA2 jar file 'jar', plus the path to
   inputs and outputs under 'path_inp' and 'path_out' fields respectively.
   We typically execute the workflow on a multi-core CPU system using
   the following command by specifying the number of cores to be used
   "–cores [=all]" and the rule name:

```
$ snakemake --cores all rule_name
```

   Please consult the Snakemake documentation for further details (see
   `https://snakemake.readthedocs.io/en/stable/`).

Use Case 1: Comparison of wild-type and knock-out samples

The JACUSA2 workflow detects RNA modifications using direct RNA se-
quencing by comparing modified samples to unmodified control samples.

10

Here, we used a published dataset of HEK293 cell lines to map m6A modification [Pratanwanich et al., 2021]. Our examples encompasses two conditions: wild-type RNA (WT, modified RNAs) and RNA from *METTL3* knockout cells (KO, m6A modification is absentr). We use two replicates per condition (see `https://doi.org/10.5281/zenodo.5913452`). The FASTQ files are mapped using Minimap2 as described in the previous section. The following analysis is validated against m6A sites consistently reported in three miCLIP-based studies Boulias et al. [2019], Koh et al. [2019], Körtel et al. [2021] (Figure 5).

Starting with the preprocessed mapped reads as inputs (BAM files), 'HEK293T-WT-rep2.bam' and 'HEK293T-WT-rep3.bam' represent the wild-type replicates and 'HEK293T-KO-rep2.bam' and 'HEK293T-KO-rep3.bam' the control replicates,

1. Compute read error profile with the `jacusa2_call2` rule:

   ```
   $ snakemake --cores all jacusa2_call2  $
   ```

   The method requires BAM files of the paired conditions and the corresponding library information "-P1" and "-P2". In addition to the mismatch score, add "-D" and "-I" to output the deletion and insertion scores. JACUSA2 allows filtering reads according to many parameters. Here, we consider all sites with base calling quality "-q [> 1]", mapping quality "-m [> 1] and read coverage "-c [> 4]". Here, we consider filtering sites within homopolymer regions "-a [=Y]". The output (named here, "Cond1vsCond2Call2.out") consists of a read error profile where the format is a combination of BED6 with JACUSA2 call-2 specific columns and common info columns: info, filter, and ref. Check JACUSA2 manual for more details on JACUSA2 filter and output options [JAC, 2021]. The number of threads can be customized via the parameter "-p". All parameters related to the JACUSA2 method can be added under the field "jacusa_params" in the config file by setting the name of the parameter followed by the corresponding value [key: value]. Be aware to set all parameters before running the pipeline.

2. Process JACUSA2 output with the `get_features` rule:

   ```
   $ snakemake --cores all get_features
   ```

   we select all sites within 5-mer of a central nucleotide 'A' flanked by 2 random nucleotides (NNANN) and we filter out sites of the homopolymer regions. Then, we rebuild the tabular features such that the observations are only sites with a reference base 'A'. Each site is characterized by 15 features corresponding to the mismatch, insertion and deletion scores for the observed site and its two flanking positions from both sides. The rule "get_features" performs the preprocessing

11

step. Use the parameter 'region' with a file containing target 5-mers to limit the analysis to specific sites. The output is an R object "features/features.rds", representing the matrix of Sites×15 features.

3. Extract characteristic m6A modification patterns with the `get_pattern` rule:

```
$ srun snakemake --cores all get_pattern
```

We learn a model representing the m6A modification patterns given the matrix of Sites×Features. To this end, we employ non-negative matrix factorization (NMF)[Lee and Seung, 1999]. Briefly, NMF factorizes a non-negative data matrix X (here: n sites and m features) into two non-negative matrices as $X \approx WH$, such that W is an $n \times k$ matrix containing basis vectors and H is an $k \times m$ matrix containing coefficient vectors. The coefficient vectors and their combination can be viewed as a pattern for m6A modification. The rank of factorization k is a critical parameter that affects the performance substantially. We suggest to select the rank k according to the method of Frigyesi and Höglund [2008] by looking at silhouette [Rousseeuw, 1987] and cophenetic correlation [Brunet et al., 2004] indices. Accordingly, the performance indices are computed for different choices of rank ($k < n, m$) and compared to the performance of a random permutation of the original data. Subsequently, the chosen rank corresponds to the value with the largest difference between slopes of the original and the randomized data. Here, the unsupervised pattern training is based on the consensus set of $1,905$ m6A sites reported in the three miCLIP-based studies mentioned earlier. Based on the silhouette and cophenetic correlation indices, we identified an optimal factorization rank of 6 (Figure 6A). We then analyzed the identified patterns. According to the membership indicator of each site in matrix W, more than 80% of m6A modification sites can be represented by five patterns (Patterns 1,2,3,4,6) (Figure 6B). Interestingly, the linear combination of these five patterns in Figure 6C highlights the importance of position 3.

Multiple patterns and their combinations can be visualized using `visualize_pattern` rule. The corresponding outputs are under "pattern/viz" folder.

```
$ srun snakemake --cores all visualize_pattern
```

4. Predict m6A modifications with the `predict_modification` rule:

```
$ srun snakemake --cores all predict_modification
```

This rule uses patterns of 15 features to predict m6A modification. We examine the ability of prediction on a subset of data of more than

12

1.52 million sites including $17,021$ miCLIP m6A sites. We opt for the linear combination of the five most relevant patterns described in step 3. The empirical Cumulative Distribution Function (eCDF) of the inferred scores shows a significant difference between the different miCLIP m6A categories (miCLIP annotation) and the unmodified sites (Figure 6D). As the number of negative samples is much larger than the number of positive samples, we consider the Positive Predictive Value (PPV, TP/(TP+FP)) of our predictions. Here, Figure 6E shows that PPV increases with the score cut-off. The final output is a BED file containing the estimated scores as well as the corresponding eCDF and PPV plots. The corresponding outputs are located under a new folder called "prediction".

Use Case 2: Comparison of wild-type and IVT samples

An alternative way to detect RNA modifications is to compare a modified sample to an *in-vitro* transcribed (IVT) control sample. Therefore, we benchmark JACUSA2 on a sample set of two replicates from wild-type HEK293 cell lines (see Use Case 1m modified sample) Pratanwanich et al. [2021] and a modification-free IVT sample from HEK293 cDNA (control sample) (see "Preparation of an *in vitro* transcriptome sample"). All analysis steps are identical to use case 1. We evaluate the analysis against miCLIP m6A sites (Figure 5).

1. Identify read error profile: we use JACUSA2 call-2 with the same parameters as the previously described case. The input BAM files (HEK293T-WT-rep2.bam, HEK293T-WT-rep3.bam) and (HEK293T-IVT-rep1.bam, HEK293T-IVT-rep2.bam) are associated to the wild-type and IVT replicate samples respectively. All input files are available from `https://doi.org/10.5281/zenodo.5913452`

   ```
   $ srun snakemake --cores all jacusa2_call2
   ```

2. Process JACUSA2 output: we consider all sites corresponding to a 5-mer (NNANN) with a central A residue. We employ the Y filter to excludes sites within homo-polymer regions.

   ```
   $ srun snakemake --cores all get_features
   ```

3. Extract m6A modification pattern: Based on the silhouette and cophenetic correlation indices, we identified an optimal factorization rank of 6 (Figure 7A). We determined the predominant factors from matrix W. Accordingly, more than 80% of m6A modification sites can be represented by four patterns (Patterns: 1,2,3,6) (Figure 7B). In agreement with Use Case 1, the linear combination of the four patterns

13

confirms the importance of position 3 and the implication of all scores as shown in Figure 7C.

```
$ srun snakemake --cores all get_pattern
```

4. Predict m6A modifications: we evaluate the prediction ability of the detected patterns on a test set of almost $1,52$ million sites where $17,021$ are miCLIP-m6A modified. We consider the linear combination of the four most relevant patterns (1,2,3,6). Figure 7D shows the eCDF of the inferred scores. The difference between the cumulative distribution of non miCLIP sites and miCLIP sites can be nicely observed, while the PPV plot shows a lower performance as compared to Use Case 1 (Figure 7E). The decrease in performance is likely explained by the absence of all modifications in the IVT samples. Additional adenosine modifications such as RNA editing may be counted as false positives.

```
$ srun snakemake --cores all predict_modification
```

NOTES

Tips and Tricks

1. The reverse transcription step during library preparation is optional. However, we recommend to include this step to ensure proper sequencing also of RNAs with secondary structures. Superscript IV reverse transcriptase may be replaced by Superscript III reverse transcriptase, which is used in the protocol provided by Oxford Nanopore Technologies.

2. The library preparation protocol contains two bead clean up steps. It is important to remove ethanol and wash buffer completely. However, beads should not be dried for several minutes. Directly add water or elution buffer after washing to prevent sticking of the RNA to the beads.

3. The default filter in current MinKNOW versions is a Q score of 9. For direct RNA sequencing we recommend to adjust the output filter to a minimum Q score of 7, as in previous MinKNOW versions.

4. During preparation of the *in vitro* transcriptome sample, *in vitro* transcription and clean up kits may be replaced by equivalent products. The protocol however has been tested only with the mentioned kits.

5. Configuration of the pipeline should be handled via the config file: `config.yaml`. All parameters should be set before executing rules.

6. Once the pipeline has run successfully you should expect the following folders with the corresponding outputs in the output directory: bam, jacusa, features, patterns, and prediction.

7. JACUSA2 call2 could be run separately using the command line as described in JACUSA2 manual [JAC, 2021], then put the output under a new folder with the name 'jacusa' under the output directory.

8. In the snakemake pipeline, rules are linked so that the workflows are determined from top (e.g. predict_modification) to bottom (e.g. sort_bam) and executed accordingly from bottom to top (Figure 4). Therefore, running for example "predict_modification" rule leads to executing all rules on its pipeline.

9. This workflow uses a subset of the input data that correspond to known modified sites to derive characteristic read alignment profiles by NMF (patterns). Alternatively, predefined patterns could be used via a preloaded NMF R object to compute scores for modification site prediction.

ACKNOWLEDGMENTS

REFERENCES

Minimap2. `https://github.com/lh3/minimap2`. Accessed: 2022-01-19.

Jacusa2 manual. `https://github.com/dieterich-lab/JACUSA2`, 2021. Accessed: 2022-01-15.

Samir Adhikari, Wen Xiao, Yong-Liang Zhao, and Yun-Gui Yang. m(6)a: Signaling for mrna splicing. *RNA biology*, 13:756–759, September 2016. ISSN 1555-8584. doi: 10.1080/15476286.2016.1201628.

Ina Anreiter, Quoseena Mir, Jared T. Simpson, Sarath C. Janga, and Matthias Soller. New twists in detecting mrna modification dynamics. *Trends in biotechnology*, 39:72–89, January 2021. ISSN 1879-3096. doi: 10.1016/j.tibtech.2020.06.002.

Konstantinos Boulias, Diana Toczydłowska-Socha, Ben R Hawley, Noa Liberman, Ken Takashima, Sara Zaccara, Théo Guez, Jean-Jacques Vasseur, Françoise Debart, L Aravind, et al. Identification of the m6am

methyltransferase pcif1 reveals the location and functions of m6am in the transcriptome. *Molecular cell*, 75(3):631–643, 2019.

Jean-Philippe Brunet, Pablo Tamayo, Todd R Golub, and Jill P Mesirov. Metagenes and molecular pattern discovery using matrix factorization. *Proceedings of the national academy of sciences*, 101(12):4164–4169, 2004.

Dan Dominissini, Sharon Moshitch-Moshkovitz, Schraga Schwartz, Mali Salmon-Divon, Lior Ungar, Sivan Osenberg, Karen Cesarkas, Jasmine Jacob-Hirsch, Ninette Amariglio, Martin Kupiec, Rotem Sorek, and Gideon Rechavi. Topology of the human and mouse m6a rna methylomes revealed by m6a-seq. *Nature*, 485:201–206, April 2012. ISSN 1476-4687. doi: 10.1038/nature11112.

Hao Du, Ya Zhao, Jinqiu He, Yao Zhang, Hairui Xi, Mofang Liu, Jinbiao Ma, and Ligang Wu. Ythdf2 destabilizes m 6 a-containing rna through direct recruitment of the ccr4–not deadenylase complex. *Nature communications*, 7(1):1–11, 2016.

Attila Frigyesi and Mattias Höglund. Non-negative matrix factorization for the analysis of complex gene expression data: identification of clinically relevant tumor subtypes. *Cancer informatics*, 6:CIN–S606, 2008.

David Garcias Morales and José L. Reyes. A birds'-eye view of the activity and specificity of the mrna m, javax.xml.bind.jaxbelement@6d66739e, a methyltransferase complex. *Wiley interdisciplinary reviews. RNA*, 12: e1618, January 2021. ISSN 1757-7012. doi: 10.1002/wrna.1618.

Guifang Jia, Ye Fu, Xu Zhao, Qing Dai, Guanqun Zheng, Ying Yang, Chengqi Yi, Tomas Lindahl, Tao Pan, Yun-Gui Yang, and Chuan He. N6-methyladenosine in nuclear rna is a major substrate of the obesity-associated fto. *Nature chemical biology*, 7:885–887, October 2011. ISSN 1552-4469. doi: 10.1038/nchembio.687.

Shengdong Ke, Endalkachew A. Alemu, Claudia Mertens, Emily Conn Gantman, John J. Fak, Aldo Mele, Bhagwattie Haripal, Ilana Zucker-Scharff, Michael J. Moore, Christopher Y. Park, Cathrine Broberg Vågbø, Anna Kuśnierczyk, Arne Klungland, James E. Darnell, and Robert B. Darnell. A majority of m6a residues are in the last exons, allowing the potential for 3' utr regulation. *Genes & development*, 29:2037–2053, October 2015. ISSN 1549-5477. doi: 10.1101/gad.269415.115.

Casslynn WQ Koh, Yeek Teck Goh, and WS Sho Goh. Atlas of quantitative single-base-resolution n 6-methyl-adenine methylomes. *Nature communications*, 10(1):1–15, 2019.

Nadine Körtel, Cornelia Rücklé, You Zhou, Anke Busch, Peter Hoch-Kraft, Reymond FX Sutandy, Jacob Haase, Mihika Pradhan, Michael Musheev, Dirk Ostareck, et al. Deep and accurate detection of m6a rna modifications using miclip2 and m6aboost machine learning. *bioRxiv*, pages 2020–12, 2021.

Johannes Köster and Sven Rahmann. Snakemake—a scalable bioinformatics workflow engine. *Bioinformatics*, 28(19):2520–2522, 2012.

Daniel D Lee and H Sebastian Seung. Learning the parts of objects by non-negative matrix factorization. *Nature*, 401(6755):788–791, 1999.

Kate D. Meyer, Yogesh Saletore, Paul Zumbo, Olivier Elemento, Christopher E. Mason, and Samie R. Jaffrey. Comprehensive analysis of mrna methylation reveals enrichment in 3' utrs and near stop codons. *Cell*, 149: 1635–1646, June 2012. ISSN 1097-4172. doi: 10.1016/j.cell.2012.05.003.

Deepak P Patil, Brian F Pickering, and Samie R Jaffrey. Reading m6a in the transcriptome: m6a-binding proteins. *Trends in cell biology*, 28(2): 113–127, 2018.

Michael Piechotta, Qi Wang, Janine Altmüller, and Christoph Dieterich. Rna modification mapping with jacusa2. *bioRxiv*, 2021.

Ploy N Pratanwanich, Fei Yao, Ying Chen, Casslynn WQ Koh, Yuk Kei Wan, Christopher Hendra, Polly Poon, Yeek Teck Goh, Phoebe ML Yap, Jing Yuan Chooi, et al. Identification of differential rna modifications from nanopore direct rna sequencing with xpore. *Nature Biotechnology*, 39(11):1394–1402, 2021.

Jean-Yves Roignant and Matthias Soller. m, javax.xml.bind.jaxbelement@8cec19d, a in mrna: An ancient mechanism for fine-tuning gene expression. *Trends in genetics : TIG*, 33: 380–390, June 2017. ISSN 0168-9525. doi: 10.1016/j.tig.2017.04.003.

Ian A. Roundtree, Molly E. Evans, Tao Pan, and Chuan He. Dynamic rna modifications in gene expression regulation. *Cell*, 169:1187–1200, June 2017. ISSN 1097-4172. doi: 10.1016/j.cell.2017.05.045.

Peter J Rousseeuw. Silhouettes: a graphical aid to the interpretation and validation of cluster analysis. *Journal of computational and applied mathematics*, 20:53–65, 1987.

Hailing Shi, Jiangbo Wei, and Chuan He. Where, when, and how: Context-dependent functions of rna methylation writers, readers, and erasers. *Molecular cell*, 74:640–650, May 2019. ISSN 1097-4164. doi: 10.1016/j.molcel.2019.04.025.

Xiao Wang, Zhike Lu, Adrian Gomez, Gary C Hon, Yanan Yue, Dali Han, Ye Fu, Marc Parisien, Qing Dai, Guifang Jia, et al. N 6-methyladenosine-dependent regulation of messenger rna stability. *Nature*, 505(7481):117–120, 2014.

Xiao Wang, Boxuan Simen Zhao, Ian A Roundtree, Zhike Lu, Dali Han, Honghui Ma, Xiaocheng Weng, Kai Chen, Hailing Shi, and Chuan He. N6-methyladenosine modulates messenger rna translation efficiency. *Cell*, 161(6):1388–1399, 2015.

Sara Zaccara, Ryan J. Ries, and Samie R. Jaffrey. Reading, writing and erasing mrna methylation. *Nature reviews. Molecular cell biology*, 20:608–624, October 2019. ISSN 1471-0080. doi: 10.1038/s41580-019-0168-5.

Zhang Zhang, Tao Chen, Hong-Xuan Chen, Ying-Yuan Xie, Li-Qian Chen, Yu-Li Zhao, Biao-Di Liu, Lingmei Jin, Wutong Zhang, Chang Liu, et al. Systematic calibration of epitranscriptomic maps using a synthetic modification-free rna library. *Nature Methods*, 18(10):1213–1222, 2021.

Guanqun Zheng, John Arne Dahl, Yamei Niu, Peter Fedorcsak, Chun-Min Huang, Charles J. Li, Cathrine B. Vågbø, Yue Shi, Wen-Ling Wang, Shu-Hui Song, Zhike Lu, Ralph P. G. Bosmans, Qing Dai, Ya-Juan Hao, Xin Yang, Wen-Ming Zhao, Wei-Min Tong, Xiu-Jie Wang, Florian Bogdan, Kari Furu, Ye Fu, Guifang Jia, Xu Zhao, Jun Liu, Hans E. Krokan, Arne Klungland, Yun-Gui Yang, and Chuan He. Alkbh5 is a mammalian rna demethylase that impacts rna metabolism and mouse fertility. *Molecular cell*, 49:18–29, January 2013. ISSN 1097-4164. doi: 10.1016/j.molcel.2012. 10.015.
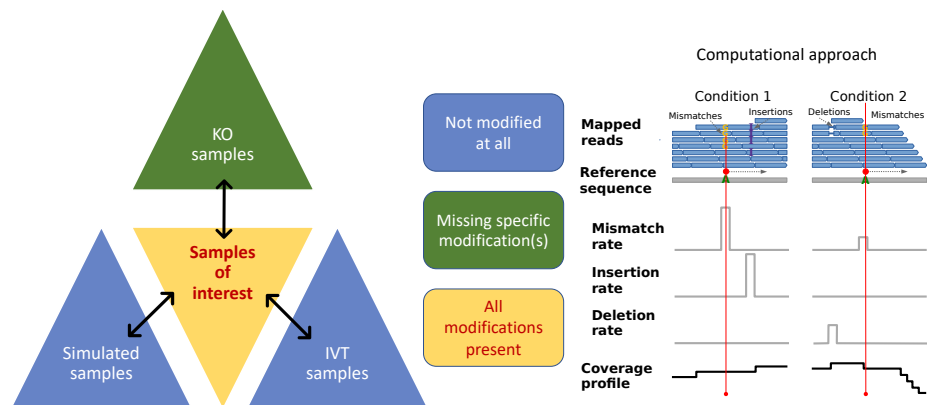
FIGURES

Figure 1: **General outline of RNA modification detection by JA-CUSA2.** A key feature of our approach is that multiple replicates of the same condition can be considered simulatenously. Samples of interests where all modifications are present could be compared with either KO samples where the modification of interest is missing or IVT/simulated samples where all modifications are absent (left panel). Read stacks (in blue) are compared head-to-head as shown on the right.
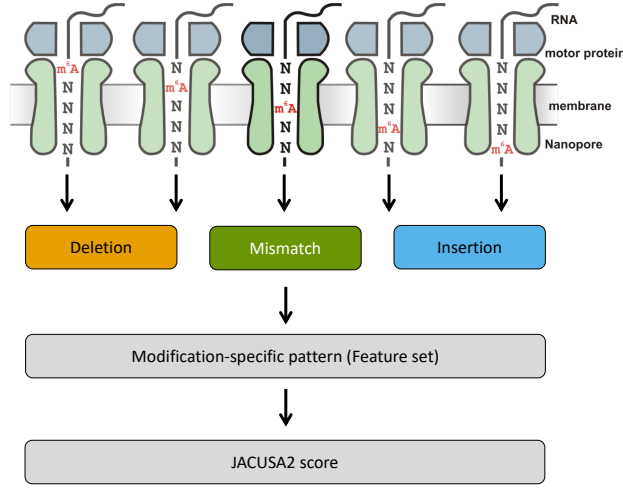
Figure 2: **Motivation of 5-mer context for RNA modification mapping**. The nanopore covers 5 consecutive RNA residues. That is why we consider a 5-mer context and derive 3 principal features for every position within a given 5-mer (15 features in total, with a central A residue in this example). We evaluate each feature set by previously learned patterns and compute a final score for modification site detection.
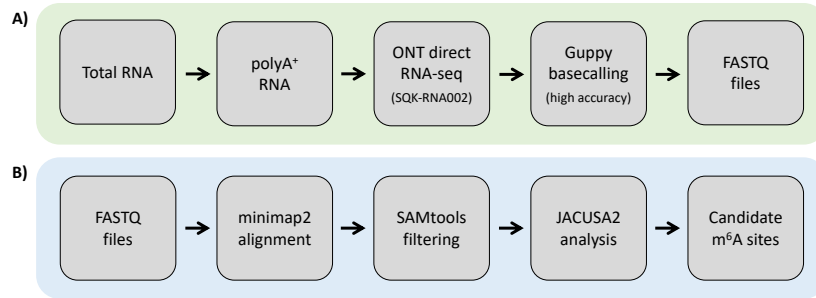
Figure 3: **Experimental and computational workflow**. A) Starting from total cellular RNA, polyA$^+$ RNA is isolated and subjected to Nanopore direct RNA-sequencing. Guppy basecalling can be done as live basecalling during sequencing or after the sequencing run from generated FAST5 files, resulting in FASTQ output files. B) FASTQ files are aligned to a reference sequence with Minimap2. SAMtools is used to generate BAM files as input for JACUSA2 analysis, which yields candidate m6A sites as described in Figure 4.
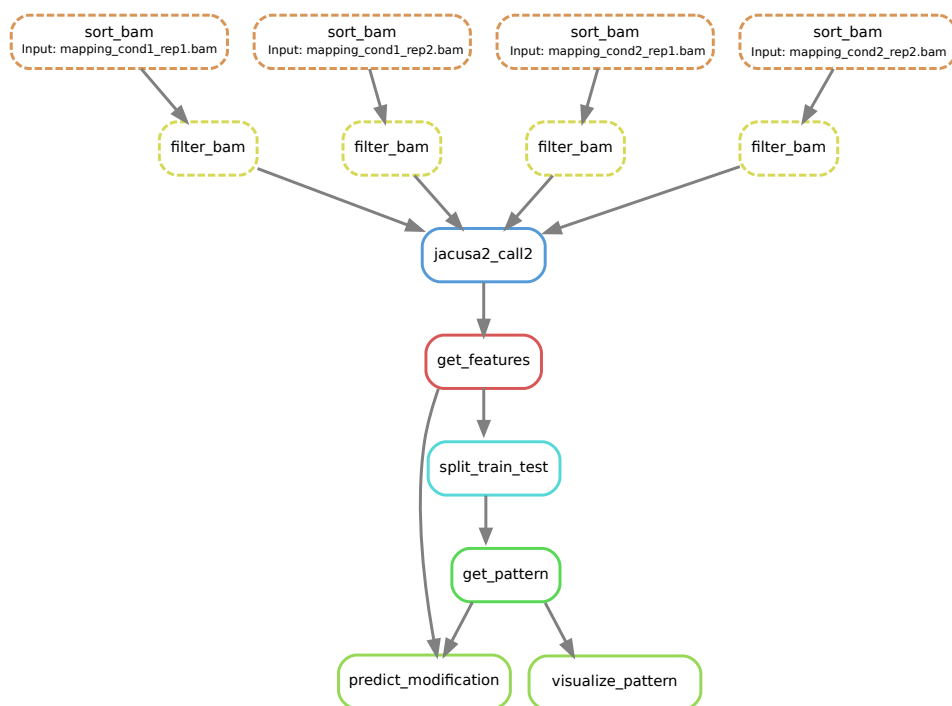
Figure 4: **Computational workflow**. Snakemake workflow for RNA modification detection based on JACUSA2 variant calling.
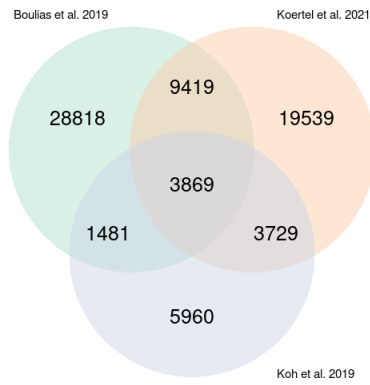
Boulias et al. 2019

Koertel et al. 2021

9419

28818

19539

3869

1481

3729

5960

Koh et al. 2019

Figure 5: **m6A sites reported in the three miCLIP-based studies** Boulias et al. [2019], Koh et al. [2019] and Körtel et al. [2021].

TABLES

Software	Version	Description
Minimap2	`https://github.com/lh3/minimap2` v2.22 or later	`https://lh3.github.io/minimap2/`
samtools	`https://github.com/samtools/` `samtools` v1.12 or later	`http://samtools.github.io/`
JAVA	`https://openjdk.java.net/` 11.0.12 2021-07-20 - JAVA 11 or later	OpenJDK Runtime Environment
R	`https://www.r-project.org/` version 3.5.1 or later	The R Project for Statistical Computing
PERL	`https://www.perl.org/` version 5.28.1 or later	Perl is a highly capable, feature-rich programming language
bedtools	`https://github.com/arq5x/bedtools2` version 2.29.2 or later	Perl is a highly capable, feature-rich programming language
snakemake	`https://snakemake.github.io/` version 6.8.1 or later	The Snakemake workflow management system

Table 1: **Software dependencies**

| R Packages	Version	Description
ggplot2	`https://cran.r-project.org/web/` `packages/ggplot2/index.html` - ggplot2_3.3.0 or later	ggplot2 is a system for declaratively creating graphics, based on The Grammar of Graphics.
NMF	`https://cran.r-project.org/web/` `packages/NMF/index.html` - NMF_0.22.0 or later	Provides a framework to perform Non-negative Matrix Factorization (NMF).

Table 2: **R Package dependencies**

24
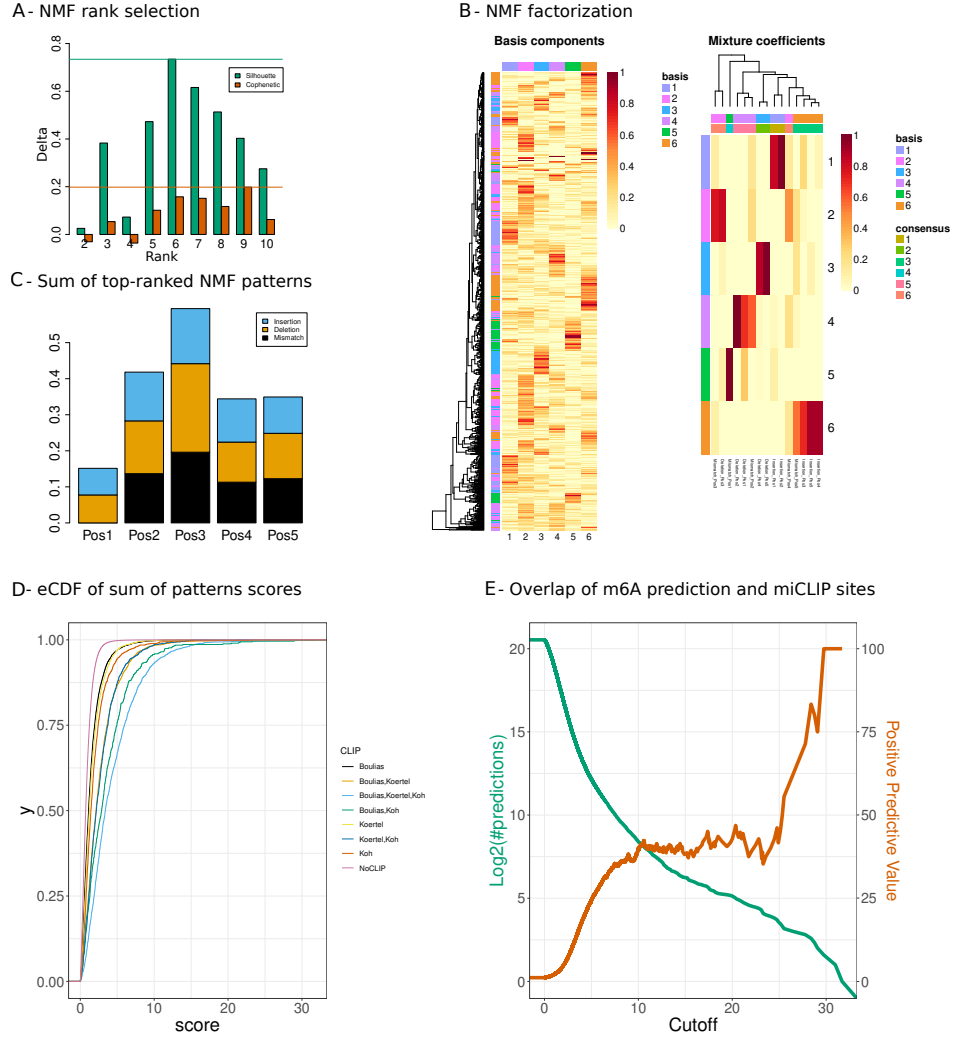
Figure 6: **Case 1. WT versus KO. A**: NMF rank selection. Barplots represent differences in cophenetic correlation and silhouette scores for NMF factorization of the original input and randomized data. Ranks with the largest differences are determined for both measures, then the smallest rank is selected for the NMF decomposition. **B**: NMF result represented by the basis matrix W ("amplitude" matrix) and the coefficient matrix H ("pattern" matrix). The matrix H induces the RNA modification pattern. **C**: Barplot shows the sum of the top 5 patterns (y-axis) across the specific 5-mer context (x-axis) and the score type: mismatch, deletion and insertion (resp. black, orange and blue). The 5 patterns (coefficient vectors: 1,2,3,4,6) are selected according to the predominant columns in matrix W. **D**: Score distribution inferred from the combined patterns, stratified by the different categories of miCLIP validated sites and non miCLIP sites. **E**: Number of predicted m6A sites (green) and Positive Predictive Value (PPV) of predicted m6A sites that overlap with miCLIP sites (orange).
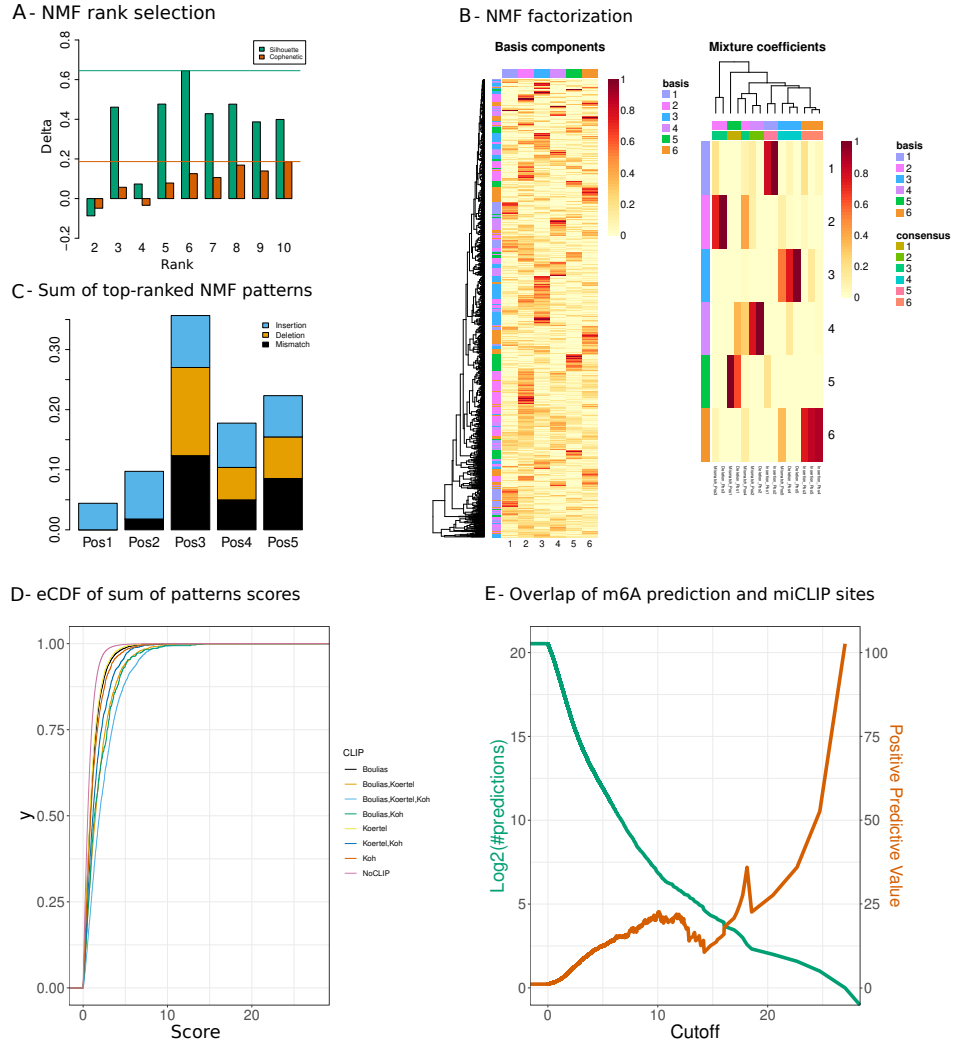
Figure 7: **Case 2. WT versus IVT. A**: NMF rank selection. Barplots represent differences in cophenetic correlation and silhouette scores for NMF factorization of the original input and randomized data. Ranks with the largest value for both indices are determined, then the smallest rank is selected for the NMF decomposition. **B**: NMF result represented by the basis matrix W ("amplitude" matrix) and the coefficient matrix H ("pattern" matrix). The matrix H induces the RNA modification pattern. **C**: Barplots representing the linear combination of the top 4 patterns (y-axis) by by the number of position in the specific 5-mer context (x-axis) and the score type: mismatch, deletion and insertion (resp. black, orange and blue). The 4 patterns (coefficient vectors: 1,2,3,6) are selected according to the predominant columns in matrix W. **D**: Score distribution inferred from the combined patterns, stratified by the different categories of miCLIP validated sites and non miCLIP sites. **E**: Number of predicted m6A sites (green) and Positive Predictive Value (PPV) of predicted m6A sites that overlap with miCLIP sites (orange).

26